

Non-hydrostatic modeling of cohesive sediment transport associated with a subglacial buoyant jet in glacial fjords: A process-oriented approach

Julio Salcedo-Castro^{a,*}, Daniel Bourgault^{b,1}, Samuel J. Bentley^{c,2}, Brad deYoung^{d,3}

^a Instituto de la Patagonia, Universidad de Magallanes, Avenida Manuel Bulnes # 01895, Punta Arenas, Chile

^b Institut des sciences de la mer de Rimouski, Université du Québec à Rimouski, 310 allée des Ursulines, Rimouski, Québec, Canada

^c Department of Geology and Geophysics, Louisiana State University, E-235 Howe-Russell, Baton Rouge, LA 70803, USA

^d Department of Physics and Physical Oceanography, Memorial University of Newfoundland, St. John's, Canada NL A1B 3X7

ARTICLE INFO

Article history:

Received 13 July 2012

Received in revised form 30 November 2012

Accepted 1 December 2012

Available online 5 January 2013

Keywords:

Glacier
Convective sedimentation
Plume
Flocculation
Buoyancy
Non hydrostatic model
Sediment dynamics
Fjord

ABSTRACT

Fine sediment transport produced by a subglacial freshwater discharge is simulated with a 2D non-hydrostatic model. The circulation pattern revealed a buoyant jet issuing from the aperture representing the subglacial tunnel, a vertically buoyant plume and a surface gravity current forming part of an estuarine circulation. Momentum-dominated experiments are more sensitive to the presence of suspended sediment in the discharge. At low concentrations, the sediment stays in the vertical plume and surface gravity current, and its concentration is progressively decreased by mixing but no settling is observed through the water column. At high concentrations, the sediment settles in the far field and is transported back to the near field by the landward estuarine current. Sediment settled from the surface layer through convective sedimentation, a process that was more effective than flocculation to transport sediment vertically, and showed vertical velocities faster than $1.0 \times 10^{-2} \text{ m s}^{-1}$. Implications of these results are discussed.

© 2012 Elsevier Ltd. All rights reserved.

1. Introduction

Approximately one-tenth of the world coastlines are active glacimarine environments or environments where sediment is deposited after being discharged from glacier ice (Curran et al., 2004). Some of these glacimarine environments are glacial fjords (ice fields or glaciers in the hinterland), characterized by high inorganic sedimentation rates, with sediment discharges coming primarily from a single source (Syvitski and Murray, 1981; Curran et al., 2004).

Especially in temperate glacial fjords, during the melting season the estuarine circulation can be idealized as a subglacial buoyant jet which transforms into a buoyant wall plume rising along the glacier face, and a gravity current at the surface or mid-depth (Syvitski, 1989; Powell, 1990; Russell and Arnott, 2003; Salcedo-Castro et al., 2011). The vertical plume has a typical horizontal length scale $L \sim 1 \text{ m}$, that is much smaller than the vertical scale of the plume which is roughly the fjord depth, i.e. $H \sim 100 \text{ m}$.

The freshwater forcing in glacial fjords is, therefore, highly non-hydrostatic because $H/L \gg 1$ (Marshall et al., 1997).

The behavior of the buoyant jet depends on the balance between the buoyancy flux, given by the density difference between the plume (ρ_0) and the ambient fluid (ρ_a), and the momentum flux, represented by the initial jet velocity u_0 . This balance between buoyancy and momentum is represented by the Froude number (Syvitski, 1989; Powell, 1990; Russell and Arnott, 2003; Salcedo-Castro et al., 2011):

$$\text{Fr} = \frac{u_0}{\left(gd \left(\frac{\rho_a - \rho_0}{\rho_0}\right)\right)^{1/2}}, \quad (1)$$

where d is the opening size, and g is the gravitational acceleration. Thus subglacial discharges can be buoyancy-dominated ($\text{Fr} < 1$) or momentum-dominated ($\text{Fr} \geq 1$) (Syvitski, 1989; Powell, 1990; Salcedo-Castro et al., 2011).

The study of buoyant jets began with the classical work of Albertson et al. (1950), Abramovic (1963), and Abraham (1969). Along with these studies, the study on buoyant plane jets was undertaken by others (Anwar, 1973; Kotsovinos, 1976; Kotsovinos, 1977; Kotsovinos and List, 1977).

The first experimental and theoretical investigations about buoyant jets in confined depth (Jirka and Harleman, 1973; Jirka,

* Corresponding author. Tel.: +56 (61) 207080.

E-mail address: j.salcedo@mun.ca (J. Salcedo-Castro).

¹ Tel.: +1 (418) 723 1986.

² Tel.: +1 (225) 578 5735.

³ Tel.: +1 (709) 864 8738.

1982; Jirka and Harleman, 1979; Lee and Jirka, 1981) stated that the structure and dilution of a buoyant jet can be defined as function of three dimensionless parameters: the Froude number Fr , the relative depth H/d (where H is the total depth) and the vertical angle of discharge (θ). Jirka and Harleman, 1973 also showed that the jet stability depended on these three parameters, where a stable jet was defined as not showing re-entrainment and recirculation cells. This dependence of the structure, stability and mixing of a buoyant jets on Fr and H/d has been observed in horizontal buoyant jets (Jirka and Harleman, 1973; Jirka, 1982; Sobey et al., 1988) and vertical buoyant jets (Jirka and Harleman, 1979; Lee and Jirka, 1981; Wright et al., 1991; Kuang and Lee, 2001, 2006).

Syvitski (1989) has pointed out that the presence of a suspended sediment load increases the initial momentum and velocity of a buoyant jet but a significant settling velocity of particles will produce a more rapid decaying of the jet velocity than that observed in a jet containing only dissolved matter. Thus it is expected that the suspended sediment will affect the buoyant discharges differently, depending on whether they are buoyancy or momentum dominated. Studies of sedimentation in glacial fjords have, however, been primarily focused on bulk sediment, so little is known about fine, cohesive, sediment transport in spite of its predominance in these systems (Syvitski, 1989; Curran et al., 2004).

Whereas suspended fine sand and coarse silt sink as single grains, the settling of finer silt and clay is affected by flocculation and the existence of aggregates (Syvitski, 1989; Curran et al., 2004). The flocculation rate is primarily dependent on sediment concentration (Mehta, 1986; Dyer, 1995; Hill et al., 1998; Hill et al., 2000; Shi and Zhou, 2004; Liu, 2005), but it is also influenced to a lesser extent by salinity, turbulence and other factors (Winterwerp, 2002; Dyer et al., 2002).

Field and laboratory studies of sedimentation from buoyant jets and plumes have been mainly focused on non-cohesive sediments, where sedimentation rate depends fundamentally on particles settling velocity (Carey et al., 1988; Sparks et al., 1991; Bursik, 1995; Ernst et al., 1996; Lane-Serff and Moran, 2005). Recently, Lane-Serff (2011) modeled the deposition of cohesive sediment from buoyant jets and found that the settling velocity decreased as the sediment load decreased. Lane-Serff also observed that the deposition rate was lower near the source but higher further away as more sediment remained in the current for longer distances.

Another process that has recently been shown to influence the sediment transport associated with buoyant plumes is the convective sedimentation (McCool and Parsons, 2004). This is produced when the stratification hinders the descent speed of the sediment and, as a result, sediment concentrates along the pycnocline, until the region becomes gravitationally unstable and the inhomogeneities in the density field turn into convective cells (Hoyal et al., 1999; Parsons and Garcia, 2001; McCool and Parsons, 2004). Laboratory observations by Green (1987) about this “sediment fingering” showed that this process can be important especially in conditions of high sediment concentration, small particles and weak stratification. Parsons et al. (2001) stated that this convection occurred even at sediment concentrations as low as 1 kg m^{-3} , and one consequence of the convective instability of the original hypopycnal plume was the generation of a bottom turbidity current, or hyperpycnal plume that moved at moderate speeds over the bottom.

There have been some modeling efforts to study the sedimentation process in glacial fjords. Mugford and Dowdeswell (2007) used a stratigraphic simulation model that could link the environmental and climatic conditions to the geological formation of distinctive glacial marine deposits in Kangerdlugssuaq Fjord (Greenland) and McBride Glacier (Alaska). More recently, Mugford and Dowdeswell (2011) used a jet model and could reproduce some important features of the sedimentation in McBride Glacier (Alaska).

Most models used in oceanography consider the hydrostatic assumption that is justified when horizontal length scales L of the motion are several orders of magnitude larger than vertical length scales H (Cushman-Roisin, 1994). Hydrostatic models, however, are not suitable to simulate highly non-hydrostatic processes such as convection and high-frequency gravity waves (Marshall et al., 1997), shelf/slope convection, and buoyancy driven coastal jets (Gallacher et al., 2001; Shaw and Chao, 2006). Here we carry out a numerical study of cohesive sediment transport associated with buoyant discharges in glacial fjords, using a non-hydrostatic model, more suitable to the nature of this processes. We hope to capture some basic understanding about the sediment transport in glacial fjords, using a simplified configuration that does not include ambient stratification, ocean currents, or ice processes.

2. Methods

2.1. Experimental setting

We used a non-hydrostatic model developed by Bourgault and Kelley (2004). This is a two-dimensional, laterally averaged model and uses a finite-difference scheme with a variable-mesh z -coordinate C -grid. The model details and experimental configuration used here are described in Bourgault and Kelley (2004) and Salcedo-Castro et al. (2011), respectively.

The module for sediment transport in the model includes an equation for the advection–diffusion of sediment concentration,

$$\frac{\partial C}{\partial t} + u \frac{\partial C}{\partial x} + (w + w_s) \frac{\partial C}{\partial z} = \frac{\partial}{\partial x} \left(\kappa_e \frac{\partial C}{\partial x} \right) + \frac{\partial}{\partial z} \left(\kappa_e \frac{\partial C}{\partial z} \right), \quad (2)$$

where $C(x, z, t)$ is the sediment concentration, $\kappa_e(x, z, t)$ is the coefficient of eddy diffusivity, and w_s is the sediment settling velocity.

The following expression is included to account for the modification of the equation of state for density by the presence of sediments (Wang et al., 2005):

$$\rho = \rho_w + \left(1 - \frac{\rho_w}{\rho_s} \right) C, \quad (3)$$

where ρ_w is the density of water, and ρ_s is the density of sediment. Also, the model includes the following bottom boundary condition to represent the processes of resuspension and deposition (Partheniades, 1965; Kuijper et al., 1989; Markofsky and Westrich, 2007):

$$\kappa_e \frac{\partial C}{\partial z} - w_s C = E_b, \quad (4)$$

where:

$$E_b = \begin{cases} E_0 \left(\frac{|\tau_b|}{\tau_c} - 1 \right) & \text{if } |\tau_b| > \tau_c \text{ (resuspension),} \\ C_b w_s \left(1 - \frac{|\tau_b|}{\tau_c} \right) & \text{if } |\tau_b| \leq \tau_c \text{ (deposition).} \end{cases} \quad (5)$$

Here, E_b is the bottom sediment flux, E_0 is the erosion coefficient, C_b is the sediment concentration at the bottom layer, and τ_c is the critical stress for resuspension and deposition. The choice of the values for the parameters used here is shown in Table 1, which was based on representative values for cohesive sediment (McAnally and Mehta, 2001; van Rijn, 2007).

Table 1
Parameters used for sediment transport in the model.

Parameter	Value
ρ_s (kg m^{-3})	2650
ρ_w (kg m^{-3})	1000
w_0 (m s^{-1})	0.00001
E_0 ($\text{kg m}^{-2} \text{s}^{-1}$)	0.0001
τ_c (Pa)	0.3

The numerical experiments were set in a two-dimensional configuration (x, z) representing a longitudinal section of a glacial fjord with the freshwater forcing at the glacier base. The glacier was represented as a vertical wall with a no-slip boundary condition. The total length of the numerical domain was 206 km, and the total depth was $H = 100$ m. The numerical grid had a constant vertical resolution of $\Delta z = 1$ m. In the horizontal, the grid had a resolution of $\Delta x = 1$ m for $0 < x < 100$ m (i.e. the region of interest). For $x > 100$ m the grid size increased linearly to a maximum of $\Delta x = 5000$ m. The domain was made very long compared to the plume width such that the seaward boundary condition did not influence the results (Fig. 1).

The initial condition was set as still, uniform-density ambient water and all simulations were run with a free surface and reached steady state in the region $x < 100$ m before the freshwater front reached the seaward boundary. The only forcing was a steady horizontal flow produced at the bottom open cells set through the glacier face. We did not vary the angle of the buoyant jet because of the simplified approach adopted in this study. In this sense, the angle of the buoyant jet is not considered relevant, as the jet momentum is rapidly lost and buoyancy has been shown to be the driving force (Salcedo-Castro et al., 2011).

2.2. Control parameters

The control parameters of the simulation were: the total depth of the fjord H , the opening size d , the jet velocity u_0 and the density difference $\Delta\rho = \rho_a - \rho_0$, where ρ_a is the ambient water density (Fig. 1).

The competing forcings that describe the jet behavior in these experiments are related to the momentum and buoyancy flux (List, 1982; Sangras et al., 1999; Jirka, 2006). The momentum flux for a plane jet is computed as:

$$M_0 = u_0^2 d, \quad (6)$$

whereas the buoyancy flux is:

$$B_0 = \frac{d u_0 g (\rho_a - \rho_0)}{\rho_0}, \quad (7)$$

By combining (6) and (7) it is possible to compare the relative predominance of momentum and buoyancy flux. The ratio:

$$l_m = \frac{M_0}{B_0^{2/3}}, \quad (8)$$

is the so-called Morton length scale (Morton, 1959). This scale represents the distance along which momentum of the buoyant jet is the predominant forcing. Beyond this distance, the jet momentum is overcome by buoyancy (Fischer et al., 1979; List, 1982).

Two non-dimensional numbers characterize the experiments. The Reynolds number:

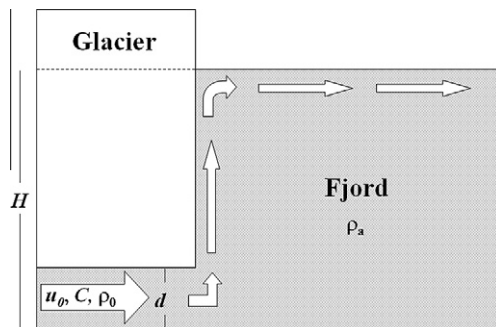


Fig. 1. Schematic representation of a glacial fjord, showing parameters considered in numerical experiments.

$$Re = \frac{u_0 d}{\nu}, \quad (9)$$

characterizes the momentum flux; and the Grashof number:

$$Gr = \frac{(\rho_a - \rho_0) g d^3}{\rho_0 \nu^2}, \quad (10)$$

characterizes the buoyancy flux, where $\nu = 1.0 \times 10^{-6} \text{ m}^2 \text{ s}^{-1}$ is the kinematic viscosity of the freshwater.

A number of experiments covering a range of buoyancy and jet dominated conditions in a glacial fjord were run. All experiments had a Re of 10^5 , whereas Gr number ranged from 10^9 and 10^{14} . The jet velocity ranged between 0.01 and 0.1 m s^{-1} , and density difference (σ_t) from 0.1 to 29.7 kg m^{-3} . Thus the Fr varied between 0.01 and 3.2 . The experimental setting and non-dimensional numbers are summarized in Table 2.

2.3. Flocculation

All runs considered the sediment grain fraction that predominates in glacial fjords, which is in the range of the silt-clay fraction (mud) (Table 3). Thus, we chose a cohesive sediment whose representative single-particle settling velocity was roughly $1.0 \times 10^{-5} \text{ m s}^{-1}$ (very fine silt-coarse clay with grain density of $\sim 2650 \text{ kg m}^{-3}$) (Mehta, 1989; Cheng, 1997). However, sediment of this grain size generally exists in flocculated form in the marine environment. Therefore, it was necessary to represent the process of flocculation in the model.

To represent flocculation, we used three ranges of concentration and the well-established power-law relationship between sediment concentration and settling velocity (Mehta, 1986). When the sediment concentration are very low, there is no flocculation and the sediment settles with single-particle settling velocity (Eq. (11a)). As sediment concentration increases, the sediment particles flocculate and settle with a concentration-dependent velocity (Eq. (11b)). When the sediment concentration reaches a threshold value, the settling velocity decreases due to particles hindrance (Richardson and Zaki, 1954; Mehta, 1986; Puls et al., 1988) (Eq. (11c)):

$$w_s = \begin{cases} w_0 & \text{if } C \leq 8.6 \times 10^{-3} \text{ kg m}^{-3} & \text{(a)} \\ k_1 C^n & \text{if } 8.6 \times 10^{-3} < C \leq 1.7 \text{ kg m}^{-3} & \text{(b)} \\ w_{s0} (1 - k_2 C)^\beta & \text{if } C > 1.7 \text{ kg m}^{-3} & \text{(c)} \end{cases} \quad (11)$$

It is worth mentioning, however, that this is a “proxy representation of flocculation”, since it does not include any aggregation or break-up behavior between cohesive particles and flocs.

In these expressions for the settling velocity, k_1 , k_2 , n and β are empirical constants, w_0 represents the individual particle settling velocity, and w_{s0} is a threshold particle velocity before observing hindrance. We set these values based on representative values for cohesive sediment from literature (Puls et al., 1988; Van Leusen, 1988; Mehta, 1989; Burt, 1986; Spearman and Roberts, 2002; Shi and Zhou, 2004). The setting for flocculation is shown in Table 4. The parameters set in Table 4 result in a maximal settling velocity of $2.4 \times 10^{-3} \text{ m s}^{-1}$, which is in the range observed in the field (Hill et al., 1998; Shi and Zhou, 2004). The dependence of settling velocity on sediment concentration is linear up to a concentration of 1.7 kg m^{-3} (Fig. 2).

By modifying the initial jet velocity and density difference, a number of experiments covering a range from buoyancy to momentum dominated conditions were run. These experiments encompassed a range of Fr between 0.01 and 3.2 . Four sediment concentrations were set: 0.01 , 0.1 , 1 , and 10 kg m^{-3} . The upper

Table 2
Control parameters and non-dimensional numbers for experiments of subglacial freshwater discharges.

Run	d (m)	u_0 (m s ⁻¹)	$\Delta\rho$ (kg m ⁻³)	Re	Gr	Fr	B_0 (s ⁻³ s ⁻³)	M_0 (s ⁻³ s ⁻²)	l_m (m)
1	1	0.1	0.102	1.0×10^5	1.0×10^9	3.2	1.0×10^{-4}	1.0×10^{-2}	4.64
2	1	0.1	1.019	1.0×10^5	1.0×10^{10}	1.0	1.0×10^{-3}	1.0×10^{-2}	1.00
3	1	0.1	10.194	1.0×10^5	1.0×10^{11}	0.32	9.9×10^{-3}	1.0×10^{-2}	0.22
4	2	0.05	12.742	1.0×10^5	1.0×10^{12}	0.10	1.2×10^{-2}	5.0×10^{-3}	0.09
5	4	0.025	15.928	1.0×10^5	1.0×10^{13}	0.030	1.5×10^{-2}	2.5×10^{-3}	0.04
6	7	0.014	29.719	1.0×10^5	1.0×10^{14}	0.010	2.8×10^{-2}	1.4×10^{-3}	0.02

Table 3
Typical values of sediment concentration and grain size found in glacial fjords.

Location	Reference	Concentration range (kg m ⁻³)	Size range
Arthur Harbor, Antarctica	Ashley and Smith (2000)	0.003–0.035	Clay/silt (30:60)
MacBride Glacier, Alaska	Cowan and Powell (1990)	0.45–0.50	
MacBride Glacier, Alaska	Cowan et al. (1988)	0.5–2	99.6% < 63 μ m
Hubbard Glacier	Curran et al. (2004)	0.01–0.035	
Cierva, Brialmont, Lester Cove, Antarctica	Domack and Williams (1990)	0.0006–0.008	
Brialmont Cove, Antarctica	Domack et al. (1994)	0.00075–0.0041	2–10 μ m
Watts Glacier and Coronation-Maktak fjords	Dowdeswell (1986)		<4 μ m
Spitsbergen	Elverhøi et al. (1983)	0.02–0.5	
Kongsfjorden, Spitsbergen, Norway	Fetzer et al. (2002)		90% clay/silt (50:50)
Coronation Fjord, Baffin Island	Gilbert (1982)		30–100 μ m
Pangnirtung Fjord	Gilbert (1978)		65–90% clay/silt
Hornsund Fjord, Spitsbergen	Görlich et al. (1987)	0.01–1	
Itirbilung Fjord, Baffin Island	Hein and Syvitski (1992)		Sand/mud (50:50)
Blue Fjord, Alaska	Hoskin et al. (1978)	0.01–0.3	46–53 μ m
Muir Inlet, Alaska	Mackiewicz et al. (1984)		65–90% 4–16 μ m
Nordauslandet tidewater ice cap, Svalbard	Pfirman and Solheim (1989)	0.001–0.028	
Lange Glacier, Antarctica	Pichlmaier et al. (2004)	0.007–0.011	
Martel Inlet, Antarctica	Pichlmaier et al. (2004)	0.01–0.015	
Kongsfjorden, Svalbard, Norway	Svendsen et al. (2002)	<0.02–0.34	
Coronation Fjord, Baffin Island	Syvitski (1989)	0.01–>0.120	
Billefjorden, Svalbard	Szczuciński et al. (2009)		>90% clay/silt (50:50)
Kongsfjorden, Svalbard	Trusel et al. (2010)	0.008–0.157	
Kongsfjorden, Svalbard	Zaborska et al. (2006)	>0.3	>90% clay/silt (10:90)
Kongsfjorden, Svalbard	Zajaczkowski (2008)	0.35–0.46	

Table 4
Parameters used for flocculation in the model.

Parameter	Value
k_1	0.14
n	1.04
k_2	0.0001
w_{so} (m s ⁻¹)	0.0026
β	4.65

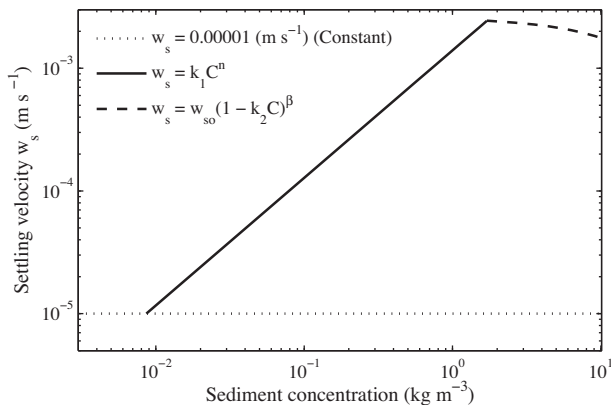


Fig. 2. Settling velocity as function of sediment concentration.

end of this range of concentrations was set according to observations made by some authors (Gilbert, 1983; Mackiewicz et al., 1984; Gilbert et al., 2002), with respect to the high concentrations found at the “upwelling zone”.

3. Results

3.1. Plume sediment concentration

The Fig. 3 shows a typical sequence of a momentum-dominated run. The initial stage of the discharge produces a horizontal jet that progresses attached to the bottom along a distance of 30 m ($t = 1081$ s and $t = 1680$ s). As the initial momentum was lost, the upper and back edges of the jet commenced to veer up and produced mushroom-like vortices ($t = 2280$ s and $t = 3481$ s). These vortices kept forming and rose along the wall ($t = 5880$ s). In response to the horizontal buoyant jet, a compensating flow toward the glacier was developed and, along with the buoyant fluid pulling the plume up, finally forced the plume to move back and rise attached to the wall. Finally, at steady-state, all experiments exhibited the same flow pattern: a buoyant jet issuing horizontally from the opening representing the subglacial tunnel, a vertical plume rising attached to the wall that produced a lifting of the sea surface when reaching the surface and a gravity surface current that set an estuarine circulation ($t = 17881$ s). Unlike the momentum-dominated discharges, the buoyancy-dominated runs went up immediately after leaving the subglacial opening but the

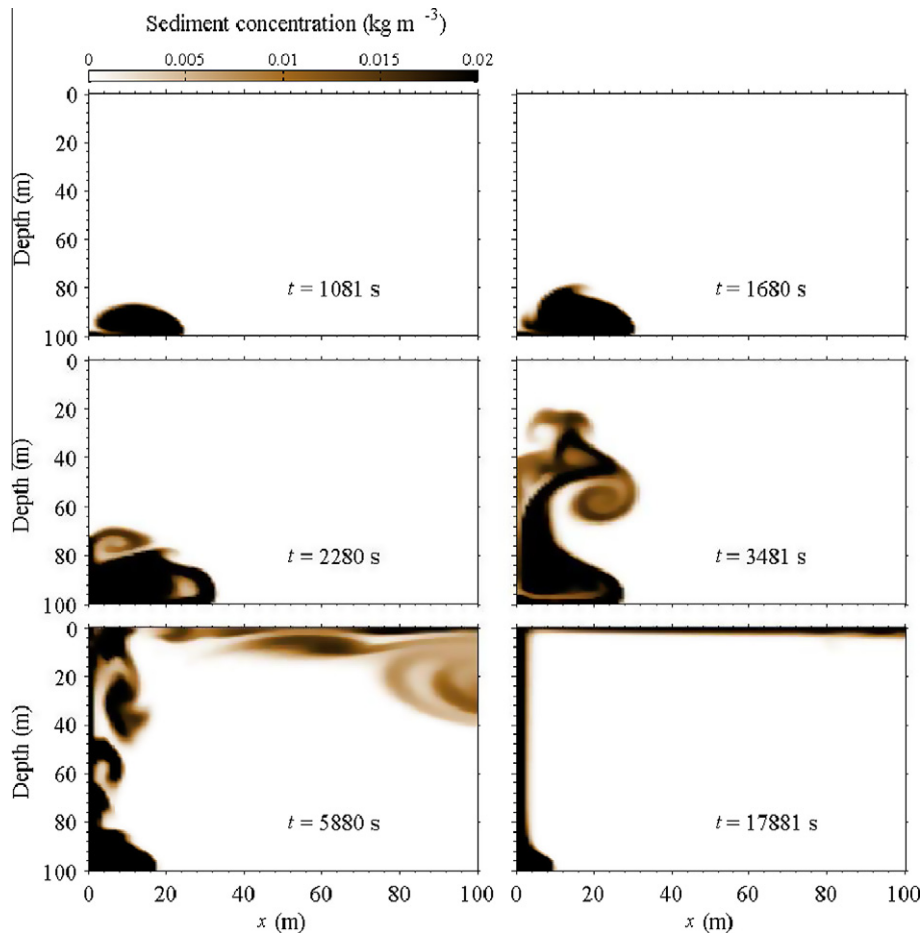


Fig. 3. Typical sequence of sediment concentration in a momentum-dominated jet issuing into the ambient denser water (run # 1, initial jet sediment concentration: 0.1 kg m^{-3}).

steady-state pattern remained qualitatively similar. This difference in the initial stage between momentum and buoyancy-dominated discharges is related to the Morton length scale (Table 2).

Flocculation did not produce any noticeable deviation of the description above for concentrations lower than 1 kg m^{-3} . In contrast, when the initial jet sediment concentration was 10 kg m^{-3} , the experiments exhibited a different pattern, where the density was more significantly affected by the presence of sediment. As the sediment concentration increased and formed a thin layer of higher subsurface sediment concentrations between 0.3 and 0.4 kg m^{-3} , at the base of the horizontal buoyant plume (Fig. 4), this thin subsurface layer became denser and unstable, as can be seen in Fig. 5. The sediment settled through the water column, in the form of finger-like extensions that came off the surface gravity current. This convective transport reached vertical velocities higher than $1.0 \times 10^{-2} \text{ m s}^{-1}$ and involved vertical sediment fluxes between 5.0×10^{-4} and $1.0 \times 10^{-3} \text{ kg m}^{-2} \text{ s}^{-1}$. In comparison, this convective settling velocity was two orders of magnitude larger than the flocculation settling velocity solely.

As sediment settled through the water column, it was carried back to the glacier by the landward lower estuarine current and re-entrained into the vertical and horizontal plumes. This estuarine current is produced as a consequence of a baroclinic pressure gradient induced by the density difference between the ambient fluid and the fresher rising plume. This condition causes surface brackish water to flow seaward whereas the underlying sea water moves toward the glacier and is also entrained into the upper layer by shear turbulence.

The maximum sediment concentration of the surface plume was determined through a vertical cross-section at distance $10d$ from the glacier. The same analysis was done for a horizontal cross-section through the vertically rising plume, at a distance $10d$ from the tunnel opening. The d dimension is the distance commonly used to compare the characteristics and self-similarity among buoyant jets. This makes sense, as the buoyancy and momentum flux depend on this dimension (Jirka and Harleman, 1973; Anwar, 1973; Kotsovinos, 1976, 1977; Kotsovinos and List, 1977).

The sediment concentration, non-dimensionalized with the initial jet sediment concentration, increased from buoyancy dominated (low Fr) to momentum dominated (high Fr) conditions in the vertical (Fig. 6(a)) and horizontal plumes (Fig. 6(b)), showing a decrease of the capacity of dilution, driven mostly by the buoyancy. When the sediment concentration at the discharge was 10 kg m^{-3} , it was possible to observe a differentiation with respect to the other experiments, due to a more marked increase in the momentum/buoyancy ratio (increasing Fr) and, consequently, an even greater decrease in their capacity of dilution.

3.2. Plume velocity

The time-averaged velocity was determined at distance $10d$ from the glacier in surface plume, and $10d$ from the tunnel opening in the vertical plume. Fig. 7 presents these mean velocities as function of the Froude number, for different sediment concentrations at the discharge. It was observed that neither the vertical plume

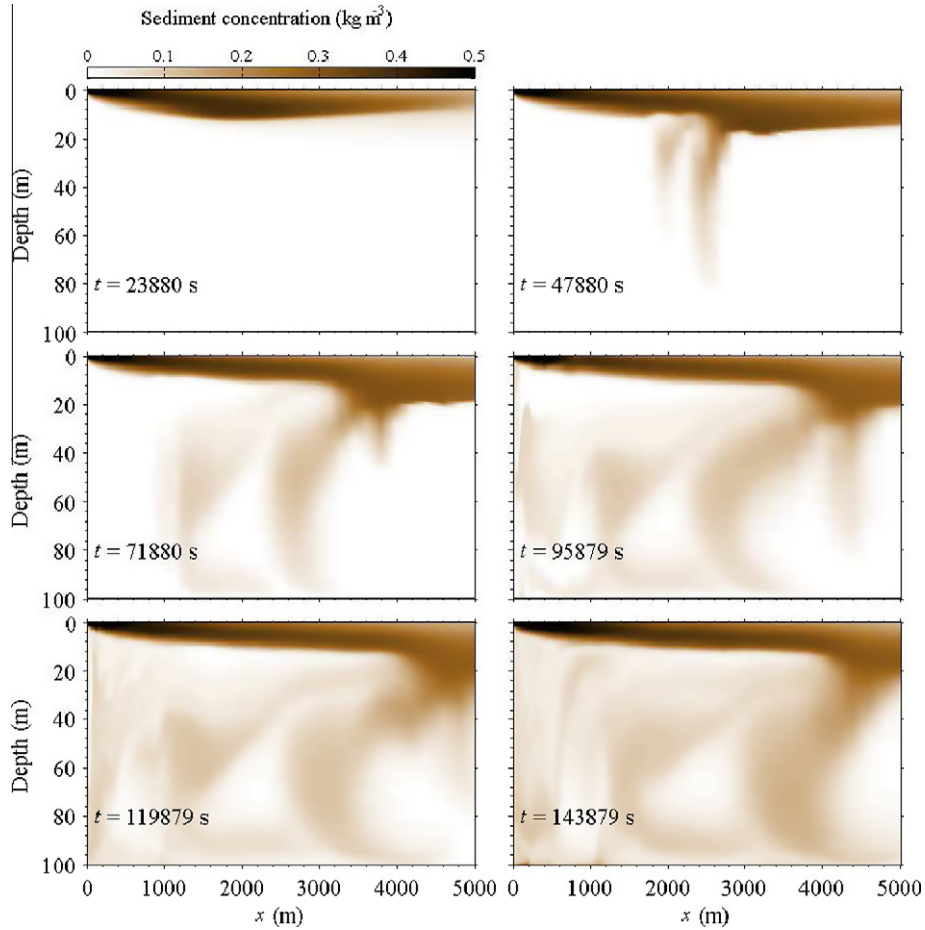


Fig. 4. Sequence of sediment concentration in the gravity plume spreading at the surface and settling of sediment in the far field (run # 3, initial jet sediment concentration: 10 kg m^{-3}).

(Figs. 7(a)) nor the horizontal surface plume (Figs. 7(b)) were affected by the presence of sediment at the discharge. As a common pattern, it was observed that all experiments decreased their velocity as the momentum/buoyancy ratio increased (higher Fr).

3.3. Plume dilution

A dilution factor (Anwar, 1973; Lee and Lee, 1998; Chen and Rodi, 1980; Huai et al., 2010) was computed to evaluate the degree of mixing along the vertical and horizontal plumes, which was defined as:

$$S = \frac{\rho_a - \rho_0}{\rho_a - \rho_p}, \quad (12)$$

where ρ_p is the plume density, at a distance equivalent to $10d$ above the opening for the vertical plume and $10d$ away from the glacier for the surface gravity plume.

Similar to the response of the plume velocity, the experiments showed an decreasing plume dilution as momentum became more important (increasing Fr) (Fig. 8). The vertical (Figs. 8(a)) and horizontal (Figs. 8(b)) plume dilution was relatively unaffected by low Fr (run # 1 and run # 2). When Fr was higher than 0.3, the experiments showed a slight trend toward higher dilution. Moreover, in spite of showing a similar trend, the experiments with initial jet sediment concentration of 10 kg m^{-3} exhibited a separation from the other runs.

4. Discussion

The addition of sediment produces a decrease in buoyancy and, consequently, a higher Fr number. This is relevant in glacial fjords because, as Salcedo-Castro et al. (2011) pointed out, the estuarine circulation in glacial fjords is primarily driven by the plume buoyancy, with the plume momentum playing a secondary role. As observed in the variations of velocity, sediment concentration and dilution, however, buoyancy still remains as the main factor controlling the fine sediment transport, and sediment produces significant changes only at relatively high concentrations.

The experiments suggest that fine sediment can be transported a long distance away of the glacier by the horizontal buoyant plume, and the sediment concentration is progressively diluted by entrainment before starting to settle through the water column. Similarly, Lane-Serff (2011) observed a lower deposition rate of cohesive sediment near the origin (compared to non-cohesive sediment) but it became higher further away from the source (as more sediment remained in the plume for longer distances).

All experiments with jet sediment concentration of 10 kg m^{-3} exhibited higher subsurface sediment concentrations at the base of the horizontal plume in the far field. This higher sediment concentration led to an instability and finally a convective transport of sediment downward through the water column. This description seems to agree well with the explanation provided by Carey et al. (1988) who asserted that the downward flux of sediment through the water column could be caused by the re-entrainment

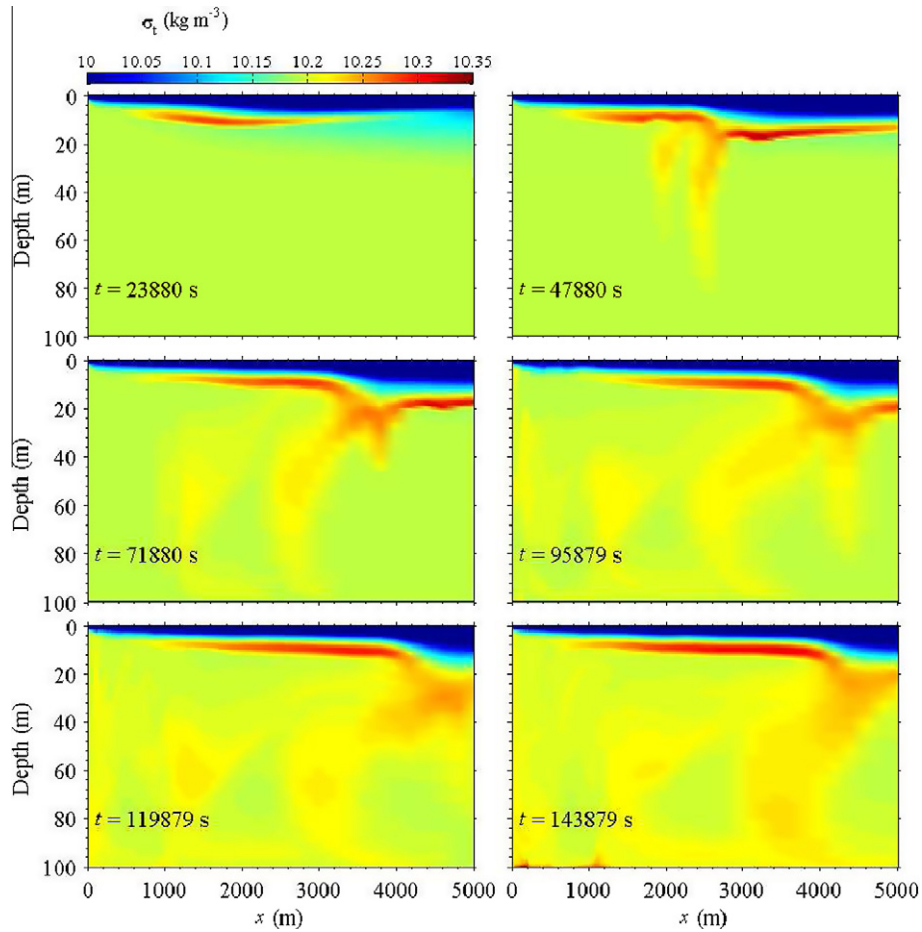


Fig. 5. Sequence of density anomaly field and changes associated with settling of sediment in the far field (run # 3, initial jet sediment concentration: 10 kg m^{-3}).

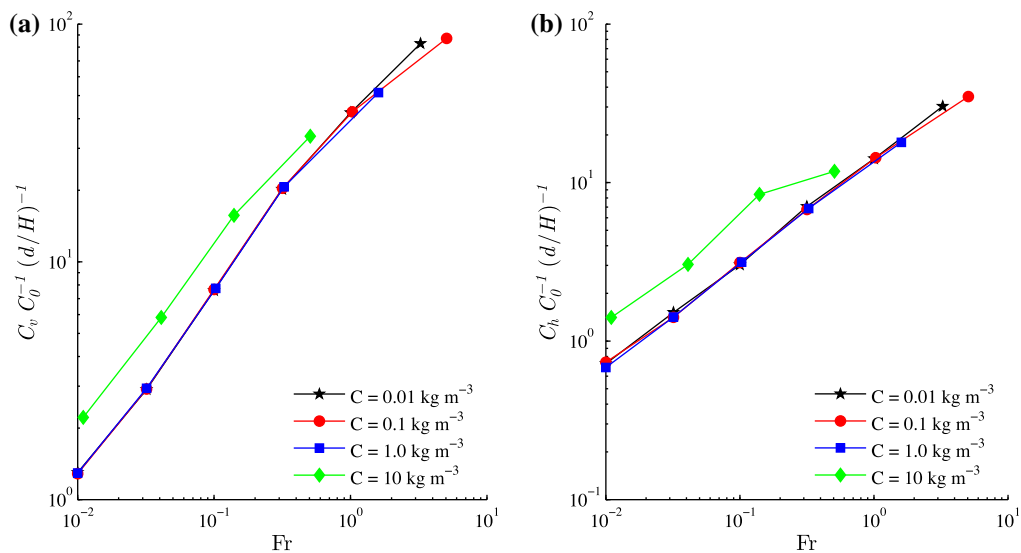


Fig. 6. Increase of non-dimensional sediment concentration in the vertical (a) and horizontal (b) plume as function of the momentum/buoyancy ratio (Fr), at a distance equivalent to $10d$, where d is the opening diameter.

of sedimenting particles in the fluid around the plume that increased the particle concentration of the plume lower margin so that the base of the plume would have a density greater than either the ambient fluid or the plume interior.

The convective transport of sediment down through the water column observed in our experiments had vertical velocities two

order of magnitude larger than those caused by flocculation. This pattern was similar to the description given by McCool and Parsons (2004), who observed convective plumes that dominated sedimentation and had vertical velocities of $1\text{--}2 \text{ cm s}^{-1}$, two orders of magnitude larger than those predicted by Stokes settling of the constituent particles. Also, surface plume concentrations as low

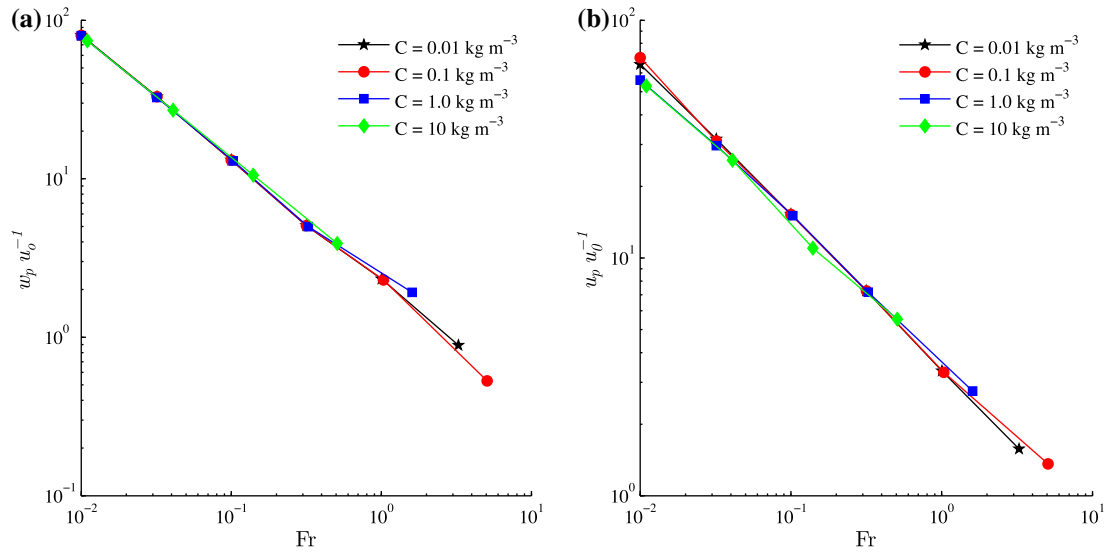


Fig. 7. Decrease of the non-dimensional velocity in the vertical (a) and horizontal (b) plume as function of the momentum/buoyancy ratio (Fr), at a distance equivalent to $10d$, where d is the opening diameter.

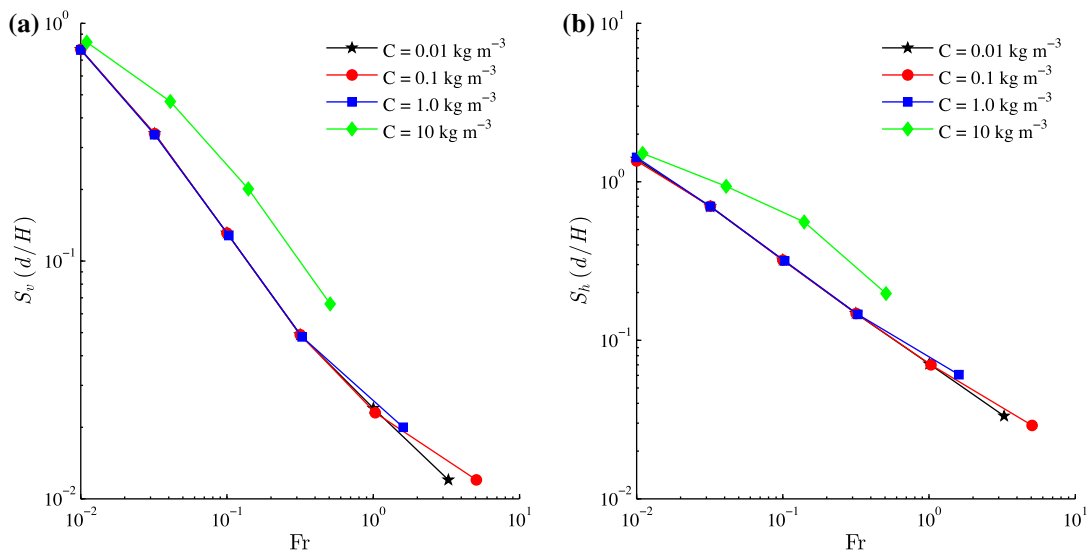


Fig. 8. Effect of sediment concentration on the vertical (a) and horizontal (b) plume dilution for different Fr numbers at a distance equivalent to $10d$, where d is the opening diameter.

as 380 mg L^{-1} (0.38 kg m^{-3}) were documented to support robust mixing-induced convective sedimentation (McCool and Parsons, 2004), which is in the same range observed in this study.

The process of sediment being carried back and re-entrained into the vertical and horizontal plumes has been described for non-cohesive sediments by other investigators. In plumes with concentrations greater than 10 g L^{-1} , Carey et al. (1988) observed the generation of dilute downward moving flows along the side of the vertical plume. Sparks et al. (1991) described an outer region where sediment falls out from the base of a horizontal turbulent gravity current and is drawn back towards the plume by a net inflow caused by the entrainment of ambient fluid as the plume rises. Ernst et al. (1996) also observed that the re-entrainment was most vigorous in runs with relatively fine-grained particles and buoyant plumes or strong jets. More recently, Cuthbertson and Davies (2008) described a tendency of settling of non-cohesive particles to be drawn back towards the margins of the rising buoyant jet and this return flow could be sufficiently strong to re-entrain

depositing particles into the rising buoyant jet. Besides, Cuthbertson et al. (2008) defined a critical distance within which particles would be re-entrained back into the rising buoyant jet, whereas those settling beyond this distance will deposit to the bed. Our results, however, showed a combination of these processes where sediment is transported from the far field back to the vertical plumes and, at the same time, part of the sediment is deposited on the bed.

The experiments with initial sediment concentrations of 10 kg m^{-3} in the issuing jet had sediment concentrations at the surface plume between 0.7 and 1 kg m^{-3} which yielded settling floc velocities of $1\text{--}1.4 \text{ mm s}^{-1}$. This range is similar to what has been observed in fjords and other estuaries by some authors. Hill et al. (1998) found that the predicted settling velocity of a 1 mm diameter floc is 1.5 mm s^{-1} . Shi and Zhou (2004) calculated settling velocities from 0.4 to 4.1 mm s^{-1} for the point-sampled data set, and from 1.0 to 3.0 mm s^{-1} for an acoustically measured data set.

There are other processes not included in this modeling and that could predominate during certain stages and in some regions of the jet and vertical and horizontal plumes. Verney et al. (2009) demonstrated that turbulent intensity is one of the main determining factors of maximum floc size. In this sense, Pejrup and Mikkelsen (2010) has shown that with the inclusion of turbulence, an improvement of up to 72% has been found in explaining the variation in settling velocity. In the same vein, Domack et al. (1994) stated that turbulent mixing near the seafloor can play an important role in the transport and break-up of floccules.

In our simulations, the background environment was considered motionless, without wind or tides that produced background turbulence. This is justified for high latitude systems where the tidal range is narrow when compared to other estuaries. In this sense, wave-associated resuspension is not considered important either, as we represented a glacial fjord adjacent to a tidewater outlet glacier where shallow areas and tidal flats are practically inexistent. Further studies should consider the inclusion of turbulence and mixing associated with waves, which is expected to produce somewhat different results. Simulations with realistic tidal forcing and stratified conditions are left to further studies.

5. Conclusion

Momentum-dominated conditions are more sensitive than buoyancy-dominated conditions to the presence of sediment in the buoyant jet discharging into the ambient water. Therefore, this type of experiments responds to even low sediment concentrations. On the other hand, buoyancy-dominated experiments exhibited noticeable changes only at high sediment concentrations and this response was less intense as buoyancy increased (Fr becoming smaller).

Cohesive sediments do not settle in the near field but are transported to the far field and settle there. These fine sediments are then carried back to the glacier and re-entrained into the vertical and horizontal plumes.

The density field is affected by the presence of sediment, as instabilities were produced by higher subsurface sediment concentrations observed at the interface between the upper and lower layer, and clouds of this denser water (and sediment) go down convectively through the water column.

Convective sedimentation proved to be a more efficient mechanism of vertical sediment transport of fine sediment, compared to individual particles settling and flocculation.

Acknowledgement

This research was carried out through the Circumpolar Flaw Lead (CFL) System Study and funded by the Canadian International Polar Year (IPY) program office and the Natural Sciences and Engineering Research Council (NSERC). We thank the anonymous reviewers for their valuable comments and suggestions.

References

Abraham, G., 1969. Horizontal jets in stagnant fluid of other density. *Journal of the Hydraulic Division, ASCE* 91, 139–153.

Abramovic, G.N., 1963. *The Theory of Turbulent Jets*. MIT Press.

Albertson, M.L., Day, Y.B., Jensen, R.A., Rouse, H., 1950. Diffusion of submerged jets. *Transactions of American Society of Civil Engineers* 115, 639–664.

Anwar, H.O., 1973. Two-dimensional buoyant jet in a current. *Journal of Engineering Mathematics* 7, 297–311.

Ashley, G.M., Smith, N.D., 2000. Marine sedimentation at a calving glacier margin. *Geological Society of America Bulletin* 112, 657–667.

Bourgault, D., Kelley, D.E., 2004. A laterally averaged nonhydrostatic ocean model. *Journal of Atmospheric and Oceanic Technology* 21, 1910–1924.

Bursik, M.I., 1995. Theory of the sedimentation of suspended particles from fluvial plumes. *Sedimentology* 42, 831–838.

Burt, T.N., 1986. Field settling velocities of mud. In: Mehta, A.J. (Ed.), *Estuarine Cohesive Sediment Dynamics, Lecture Notes on Coastal and Estuarine Studies*. Springer-Verlag, pp. 126–150.

Carey, S.N., Sigurdsson, H., Sparks, R.S.J., 1988. Experimental studies of particle-laden plumes. *Journal of Geophysical Research* 93, 15,314–15,328.

Chen, C.J., Rodi, W., 1980. *Vertical Turbulent Buoyant Jets – A Review of Experimental Data*. Pergamon Press.

Cheng, N.S., 1997. Simplified settling velocity formula for sediment particle. *Journal of Hydraulic Engineering* 123, 149–152.

Cowan, E.A., Powell, R.D., 1990. Suspended sediment transport and deposition of cyclically interlaminated sediment in a temperate glacial fjord, Alaska, U.S.A. *Geological Society, London* 53, 75–89 (special publications).

Cowan, E.A., Powell, R.D., Smith, N.D., 1988. Rainstorm-induced event sedimentation at the tidewater front of a temperate glacier. *Geology* 16, 409–412.

Curran, K., Hill, P., Milligan, T., Cowan, E., Syvitski, J., Konings, S., 2004. Fine-grained sediment flocculation below the Hubbard Glacier meltwater plume, Disenchantment Bay, Alaska. *Marine Geology* 203, 83–94.

Cushman-Roisin, B., 1994. *Introduction to Geophysical Fluid Dynamics*. Prentice Hall.

Cuthbertson, A.J.S., Davies, P.A., 2008. Deposition from particle-laden, round, turbulent, horizontal, buoyant jets in stationary and coflowing receiving fluids. *Journal of Hydraulic Engineering* 134, 390–402.

Cuthbertson, A.J.S., Apsley, D.D., Davies, P.A., Lipari, G., Stansby, P.K., 2008. Deposition from particle-laden, plane, turbulent, buoyant jets. *Journal of Hydraulic Engineering* 134, 1110–1122.

Domack, E.W., Foss, D.J.P., Syvitski, J.P.M., McClennen, C.E., 1994. Transport of suspended particulate matter in an Antarctic fjord. *Marine Geology* 121, 161–170.

Domack, E.W., Williams, C.R., 1990. Fine structure and suspended sediment transport in three Antarctic fjords. *Antarctic Research Series* 50, 71–89.

Dowdeswell, J.A., 1986. The distribution and character of sediments in a tidewater glacier, Southern Baffin Island, N.W.T., Canada. *Arctic and Alpine Research* 18, 45–56.

Dyer, K.R., 1995. Sediment transport processes in estuaries. In: Perillo, G.M.E. (Ed.), *Geomorphology and Sedimentology of Estuaries, Developments in Sedimentology*, vol. 53. Elsevier, pp. 423–449.

Dyer, K.R., Bale, A.J., Christie, M.C., Feates, N., Jones, S., Manning, A.J., 2002. The turbidity maximum in a mesotidal estuary, the Tamar estuary, UK: II. The floc properties. In: Winterwerp, J.C., Kranenburg, C. (Eds.), *Fine Sediment Dynamics in the Marine Environment*. Elsevier, pp. 219–232.

Elverhøi, A., Lønne, Ø., Seland, R., 1983. Glaciomarine sedimentation in a modern fjord environment, Spitsbergen. *Polar Research* 1, 127–149.

Ernst, G.G.J., Sparks, R.S.J., Carey, S.N., Bursik, M.I., 1996. Sedimentation from turbulent jets and plumes. *Journal of Geophysical Research* 101, 5575–5589.

Fetzer, I., Lønne, O.J., Pearson, T., 2002. The distribution of juvenile benthic invertebrates in an Arctic glacial fjord. *Polar Biology* 25, 303–315.

Fischer, H., List, E.J., Koh, R.C.Y., Imberger, J., Brooks, N.H., 1979. *Mixing in Inland and Coastal Waters*. Academic Press.

Gallacher, P.C., Piacsek, S., Dietrich, D., 2001. Hydrostatic and nonhydrostatic simulations of buoyantly driven coastal jets. In: Spaulding, M.L. (Ed.), *Proceedings of the Seventh International Conference*, November 5–7, 2001, St. Petersburg, Florida, pp. 204–214.

Gilbert, R., 1978. Observations on oceanography and sedimentation at Pangnirtung fjord, Baffin Island. *Maritime Sediments* 14, 1–9.

Gilbert, R., 1982. Contemporary sedimentary environments on Baffin Island, N.W.T., Canada: glaciomarine processes in fiords of Eastern Cumberland Peninsula. *Arctic and Alpine Research* 14, 1–12.

Gilbert, R., 1983. Sedimentary processes of Canadian Arctic fjords. *Sedimentary Geology* 36, 147–175.

Gilbert, R., Nielsen, N., Möller, H., Desloges, J.R., Rasch, M., 2002. Glaciomarine sedimentation in Kangerdluk (Disko Fjord), West Greenland, in response to a surging glacier. *Marine Geology* 191, 1–18.

Görlich, K., Węstawski, J.M., Zajaczkowski, M.J., 1987. Suspension settling effect on macrobenthos biomass distribution in the Hornsund fjord, Spitsbergen. *Polar Research* 5, 175–192.

Green, T., 1987. The importance of double diffusion to the settling of suspended material. *Sedimentology* 34, 319–331.

Hein, F.J., Syvitski, J.P.M., 1992. Sedimentary environments and facies in an arctic basin, Itirbilung Fiord, Baffin Island, Canada. *Sedimentary Geology* 81, 17–45.

Hill, P.S., Milligan, T.G., Geyer, W.R., 2000. Controls on effective settling velocity of suspended sediment in the Eel River flood plume. *Continental Shelf Research* 20, 2095–2111.

Hill, P.S., Syvitski, J.P., Cowan, E.A., Powell, R.D., 1998. In situ observations of floc settling velocities in Glacier Bay, Alaska. *Marine Geology* 145, 85–94.

Hoskin, C.M., Burrell, D.C., Freitag, G.R., 1978. Suspended sediment dynamics in Blue Fjord, Western Prince William Sound, Alaska. *Estuarine and Coastal Marine Science* 7, 1–16.

Hoyal, D.C.J.D., Bursik, M.I., Atkinson, J.F., 1999. The influence of diffusive convection on sedimentation from buoyant plumes. *Marine Geology* 159, 205–220.

Huai, W., Li, Z., Qian, Z., Zeng, Y., Han, J., 2010. Numerical simulation of horizontal buoyant wall jet. *Journal of Hydrodynamics* 22, 58–65.

Jirka, G.H., 1982. Turbulent buoyant jets in shallow fluid layers. In: Rodi, W. (Ed.), *Turbulent Buoyant Jets and Plumes*. Pergamon Press, pp. 69–120.

- Jirka, G.H., 2006. Integral model for turbulent buoyant jets in unbounded stratified flows part 2: plane jet dynamics resulting from multiport diffuser jets. *Environmental Fluid Mechanics* 6, 43–100.
- Jirka, G.H., Harleman, D.R.F., 1973. The mechanics of submerged multiport diffusers for buoyant discharges in shallow waters. Technical Report 169. Ralph M. Parsons Laboratory for Water Resources and Hydrodynamics, Massachusetts Institute of Technology, Cambridge, Massachusetts.
- Jirka, G.H., Harleman, D.R.F., 1979. Stability and mixing of a vertical plane buoyant jet in confined depth. *Journal of Fluid Mechanics* 94, 275–304.
- Kotsovinos, N.E., 1976. A note on the spreading rate and virtual origin of a plane turbulent jet. *Journal of Fluid Mechanics* 77, 305–311.
- Kotsovinos, N.E., 1977. Plane turbulent buoyant jets. Part 2. Turbulence structure. *Journal of Fluid Mechanics* 81, 45–62.
- Kotsovinos, N.E., List, E.J., 1977. Plane turbulent buoyant jets. Part 1. Integral properties. *Journal of Fluid Mechanics* 81, 25–44.
- Kuang, C.P., Lee, J.H.W., 2001. Effect of downstream control on stability and mixing of a vertical plane buoyant jet in confined depth. *Journal of Hydraulic Research* 39, 375–391.
- Kuang, C.P., Lee, J.H.W., 2006. Stability and mixing of a vertical axisymmetric buoyant jet in shallow water. *Environmental Fluid Mechanics* 6, 153–180.
- Kuijper, C., Cornelisse, J.M., Winterwerp, J.C., 1989. Research on erosive properties of cohesive sediments. *Journal of Geophysical Research* 94, 14,341–14,350.
- Lane-Serff, G.F., 2011. Deposition of cohesive sediment from turbulent plumes, gravity currents and turbidity currents. *Journal of Hydraulic Engineering* 137, 1615–1623.
- Lane-Serff, G.F., Moran, T.J., 2005. Sedimentation from buoyant jets. *Journal of Hydraulic Engineering* 131, 166–174.
- Lee, J.H.W., Jirka, G.H., 1981. Vertical round buoyant jet in shallow depth. *Journal of the Hydraulics Division, ASCE* 107, 1651–1675.
- Lee, W.T., Lee, J.H.W., 1998. Effect of lateral confinement on initial dilution of vertical round buoyant jet. *Journal of Hydraulic Engineering* 124, 263–279.
- List, E.J., 1982. Turbulent jets and plumes. *Annual Review in Fluid Mechanics* 14, 189–212.
- Liu, W.C., 2005. Modeling the influence of settling velocity on cohesive sediment transport in Tanshui River estuary. *Environmental Geology* 47, 535–546.
- Mackiewicz, N.E., Powell, R.D., Carlson, P.R., Molnia, B.F., 1984. Interlaminated ice-coximal glacial marine sediments in Muir Inlet, Alaska. *Marine Geology* 57, 113–147.
- Markofsky, M., Westrich, B., 2007. Transport modeling. In: Westrich, B., Ulrich, F. (Eds.), *Sediment Dynamics and Pollutant Mobility in Rivers. An Interdisciplinary Approach*. Springer, pp. 117–169.
- Marshall, J., Hill, C., Perelman, L., Adcroft, A., 1997. Hydrostatic, quasi-hydrostatic, and nonhydrostatic ocean modeling. *Journal of Geophysical Research* 102, 5733–5752.
- McAnally, W.H., Mehta, A.J., 2001. Seasonal variability of sediment erodibility and properties on a macrotidal mudflat, Peterstone Wentloogw, Severn estuary, UK. In: Mitchener, H.J., O'Brien, D.J. (Eds.), *Coastal and Estuarine Fine Sediment Processes*. Elsevier, pp. 301–322.
- McCool, W.W., Parsons, J.D., 2004. Sedimentation from buoyant fine-grained suspensions. *Continental Shelf Research* 24, 1129–1142.
- Mehta, A.J., 1986. Characterization of cohesive sediment properties and transport processes in estuaries. In: Mehta, A.J. (Ed.), *Estuarine Cohesive Sediment Dynamics, Lecture Notes on Coastal and Estuarine Studies*. Springer-Verlag, pp. 290–325.
- Mehta, A.J., 1989. On estuarine cohesive sediment suspension behavior. *Journal of Geophysical Research* 94, 14,303–14,314.
- Morton, B.R., 1959. Forced plumes. *Journal of Fluid Mechanics* 5, 151–163.
- Mugford, R.L., Dowdeswell, J., 2007. Numerical modelling of glacial marine sedimentation from tidewater glaciers: iceberg-rafted vs meltwater plume deposition. *Geophysical Research Abstracts* 9.
- Mugford, R.L., Dowdeswell, J.A., 2011. Modeling glacial meltwater plume dynamics and sedimentation in high-latitude fjords. *Journal of Geophysical Research*, 116.
- Parsons, J.D., Bush, J.W.M., Syvitski, J.P.M., 2001. Hyperpycnal plume formation from riverine outflows with small sediment concentrations. *Sedimentology* 48, 465–478.
- Parsons, J.D., Garcia, M.H., 2001. Enhanced sediment scavenging due to double-diffusive convection. *Journal of Sedimentary Research* 70, 47–52.
- Partheniades, E., 1965. Erosion and deposition of cohesive soils. *Journal of the Hydraulics Division* 91, 105–139.
- Pejrup, M., Mikkelsen, O.A., 2010. Factors controlling the field settling velocity of cohesive sediment in estuaries. *Estuarine, Coastal and Shelf Science* 87, 177–185.
- Pfirman, S.L., Solheim, A., 1989. Subglacial meltwater discharge in the open-marine tidewater glacier environment: observations from Nordaustlandet, Svalbard Archipelago. *Marine Geology* 86, 265–281.
- Pichlmaier, M., Aquino, F.E., Da-Silva, C.S., Braun, M., 2004. Suspended sediments in Admiralty Bay, King George Island (Antarctica). *Pesquisa Antartica Brasileira* 4, 77–85.
- Powell, R.D., 1990. Glacial marine processes at grounding-line fans and their growth to ice-contact deltas. In: Dowdeswell, J.A., Scourse, J.D. (Eds.), *Glacial Marine Environments: Processes and Sediments*, vol. 53. The Geological Society, pp. 53–73 (special publications).
- Puls, W., Kuehl, H., Heymann, K., 1988. Settling velocity of mud flocs: results of field measurements in the Elbe and the Weser estuary. In: Dronkers, J., van Leussen, W. (Eds.), *Physical Processes in Estuaries*. Springer-Verlag, pp. 404–424.
- Richardson, J.F., Zaki, W.N., 1954. The sedimentation of a suspension of uniform spheres under conditions of viscous flow. *Chemical Engineering Science* 3, 65–73.
- van Rijn, L.C., 2007. Unified view of sediment transport by currents and waves. I: initiation of motion, bed roughness, and bed-load transport. *Journal of Hydraulic Engineering* 133, 649–667.
- Russell, H., Arnott, R., 2003. Hydraulic-jump and hyperconcentrated-flow deposits of a glaciogenic subaqueous fan: Oak Ridges Moraine, Southern Ontario, Canada. *Journal of Sedimentary Research* 73, 887–905.
- Salcedo-Castro, J., Bourgault, D., deYoung, B., 2011. Circulation induced by subglacial discharge in glacial fjords: results from idealized numerical simulations. *Continental Shelf Research* 31, 1396–1406.
- Sangras, R., Dai, Z., Faeth, G.M., 1999. Mixture fraction statistics of plane self-preserving buoyant turbulent adiabatic wall plumes. *Journal of Heat Transfer* 121, 837–843.
- Shaw, P.T., Chao, S.Y., 2006. A nonhydrostatic primitive-equation model for studying small-scale processes: an object-oriented approach. *Continental Shelf Research* 26, 1416–1432.
- Shi, Z., Zhou, H.J., 2004. Controls on effective settling velocities of mud flocs in the Changjiang Estuary, China. *Hydrological Processes* 18, 2877–2892.
- Sobey, R.J., J., J.A., Keane, R.D., 1988. Horizontal round buoyant jet in shallow water. *Journal of Hydraulic Engineering* 114, 910–929.
- Sparks, R.S.J., Carey, S.N., Sigurdsson, H., 1991. Sedimentation from gravity currents generated by turbulent plumes. *Sedimentology* 38, 839–856.
- Spearman, J.R., Roberts, W., 2002. Flocculation and settling velocity of fine sediment. In: Winterwerp, J.C., Kranenburg, C. (Eds.), *Fine Sediment Dynamics in the Marine Environment*. Elsevier, pp. 277–293.
- Svendsen, H., Beszczynska-Møller, A., Hagen, J.O., Lefauconnier, B., Tverberg, V., Gerland, S., Børre-Orbæk, J., Bischof, K., Papucci, C., Zajaczkowski, M., Azzolini, R., Bruland, O., Wiencke, C., Winther, J.G., Dallmann, W., 2002. The physical environment of Kongsfjorden-Krossfjorden, an Arctic fjord system in Svalbard. *Polar Research* 21, 133–166.
- Syvitski, J.P.M., 1989. On the deposition of sediment within glacier-influenced fjords: oceanographic controls. *Marine Geology* 85, 301–329.
- Syvitski, J.P.M., Murray, J.W., 1981. Particle interaction in fjord suspended sediment. *Marine Geology* 39, 215–242.
- Szczuciński, W., Zajaczkowski, M., Scholten, J., 2009. Sediment accumulation rates in subpolar fjords-Impact of post-Little Ice Age glaciers retreat, Billefjorden, Svalbard. *Estuarine, Coastal and Shelf Science* 85, 345–356.
- Trusel, L.D., Powell, R.D., Cumpston, R.M., Brigham-Grette, J., 2010. Modern glacial marine processes and potential future behaviour of Kronebreen and Kongsvegen polythermal tidewater glaciers, Kongsfjorden, Svalbard. In: Howe, J.A., Austin, W.E.N., Forwick, M., Paetzel, M. (Eds.), *Fjord Systems and Archives*, vol. 344. Geological Society, London, pp. 89–102 (special publications).
- Van Leussen, W., 1988. Aggregation of particles, settling velocity of mud flocs. A review. In: Dronkers, J., van Leussen, W. (Eds.), *Physical Processes in Estuaries*. Springer-Verlag, pp. 347–403.
- Verney, R., Lafite, R., Brun-Cottan, J.C., 2009. Flocculation potential of estuarine particles: the importance of environmental factors and of the spatial and seasonal variability of suspended particulate matter. *Estuaries and Coasts* 32, 678–693.
- Wang, X.H., Byun, D.S., Wang, X.L., Chod, Y.K., 2005. Modelling tidal currents in a sediment stratified idealized estuary. *Continental Shelf Research* 25, 655–665.
- Winterwerp, J.C., 2002. On the flocculation and settling velocity of estuarine mud. *Continental Shelf Research* 22, 1339–1360.
- Wright, S.J., Roberts, P.J.W., Zhongmin, Y., Bradley, N.E., 1991. Surface dilution of round submerged buoyant jets. *Journal of Hydraulic Research* 29, 67–89.
- Zaborska, A., Pempkowiak, J., Papucci, C., 2006. Some sediment characteristics and sedimentation rates in an Arctic fjord (Kongsfjorden, Svalbard). *Środkowo-Pomorskie Towarzystwo Naukowe Ochrony Środowiska* 8.
- Zajaczkowski, M., 2008. Sediment supply and fluxes in glacial and outwash fjords, Kongsfjorden and Adventfjorden, Svalbard. *Polish Polar Research* 29, 59–72.